

Adsorption and stability of malonic acid on rutile TiO₂ (110), studied by near edge X-ray absorption fine structure and photoelectron spectroscopy

Karen L. Syres^{a,b,1}, Andrew G. Thomas^{a,b,*}, Darren M. Graham^{a,b,c}, Ben F. Spencer^{a,b,c}, Wendy R. Flavell^{a,b}, Mark J. Jackman^{a,b}, Vinod R. Dhanak^{d,2}

^a School of Physics and Astronomy, Alan Turing Building, The University of Manchester, Oxford Road, Manchester M13 9PL, UK

^b Photon Science Institute, Alan Turing Building, The University of Manchester, Oxford Road, Manchester M13 9PL, UK

^c Cockcroft Institute, Daresbury Laboratory, Sci-Tech Daresbury, Daresbury, Warrington WA4 4AD, UK

^d STFC Daresbury Laboratory, Sci-Tech Daresbury, Daresbury, Warrington WA4 4AD, UK

ARTICLE INFO

Article history:

Received 24 October 2013

Accepted 13 March 2014

Available online 22 March 2014

Keywords:

Titanium dioxide

Single crystal

Adsorption

Synchrotron radiation

ABSTRACT

The adsorption of malonic acid on rutile TiO₂ (110) has been studied using photoelectron spectroscopy and C K-edge, near edge X-ray fine structure spectroscopy (NEXAFS). Analysis of the O 1s and Ti 2p spectra suggest that the molecule adsorbs dissociatively in a doubly-bidentate adsorption geometry as malonate. The data are unable to distinguish between a chelating bonding mode with the backbone of the molecule lying along the [001] azimuth or a bridging geometry along the direction. Work carried out on a wiggler beamline suggests that the molecule is unstable under irradiation by high-flux synchrotron radiation from this type of insertion device.

© 2014 Elsevier B.V. All rights reserved.

1. Introduction

The interaction between carboxylic acids and TiO₂ is important in many areas of research; for example, titanium is often used for biomedical implants where the TiO₂ surface of the implant is in contact with biological molecules [1–5]. The carboxylic acid–TiO₂ interface also has importance in technological applications such as the dye-sensitised solar cell (DSSC) or Grätzel cell [6]. Since its invention, many different dyes have been investigated, most of which have relied on bonding to the TiO₂ through carboxylic acid groups [7–10]. Aranyos et al. [11] have shown that the number of attaching carboxylates on the dye influences the photoelectrochemical properties of the dye-sensitised electrode. It is also thought that the ordering of the molecules and strength of the interaction are important in the charge transfer process. In addition to the photovoltaic and biomedical applications described above, TiO₂ is a well known photocatalyst and reactions at TiO₂ surfaces are of interest in solar energy driven reactions such as water splitting

[12], production of fuels such as methanol [13] and cleaning wastewater containing organic pollutants [14].

Carboxylic acids are widely believed to attach to rutile TiO₂ (110) surfaces dissociatively via deprotonation, where the hydrogen atom is lost from the carboxylic acid group (leaving COO[−]) [15,16]. The majority of molecules then bond to the surface through the two oxygen atoms of the carboxylic acid group in a bridging bidentate structure, to two adjacent five-fold-coordinated titanium atoms on the surface [17]. Malonic acid is a simple dicarboxylic acid as shown in Fig. 1. This molecule could potentially be used as an anchoring molecule to attach any organic molecule onto a TiO₂ surface via the central CH₂ group. Such molecules could be used to functionalise the TiO₂ surface for biomedical or photovoltaic applications. Clearly for such applications the mode of bonding and the stability of the adsorbed species have some importance.

Investigating the stability of organic molecules under a synchrotron radiation X-ray beam can be very challenging. Measurements recorded at synchrotrons may provide misleading results if the molecules being investigated are damaged or break up under the beam. This is particularly important if the data acquisition time is long when damage to the molecules or photocatalysed reactions can occur in a matter of seconds. In addition, if molecules that are potentially viable for use in photovoltaic cells are unstable under the X-ray beam they may also be susceptible to long-term degradation under sunlight. Since the carboxylic acid groups usually anchor the entire dye to the TiO₂, a loss in

* Corresponding author at: School of Physics and Astronomy, Alan Turing Building, The University of Manchester, Oxford Road, Manchester M13 9PL, UK.

E-mail address: a.g.thomas@manchester.ac.uk (A.G. Thomas).

¹ Current address: The University of Nottingham, School of Chemistry, University Park, Nottingham NG7 2RD, UK.

² Current address: Physics Department and Stephenson Institute for Renewable Energy, University of Liverpool L69 7BX, UK.

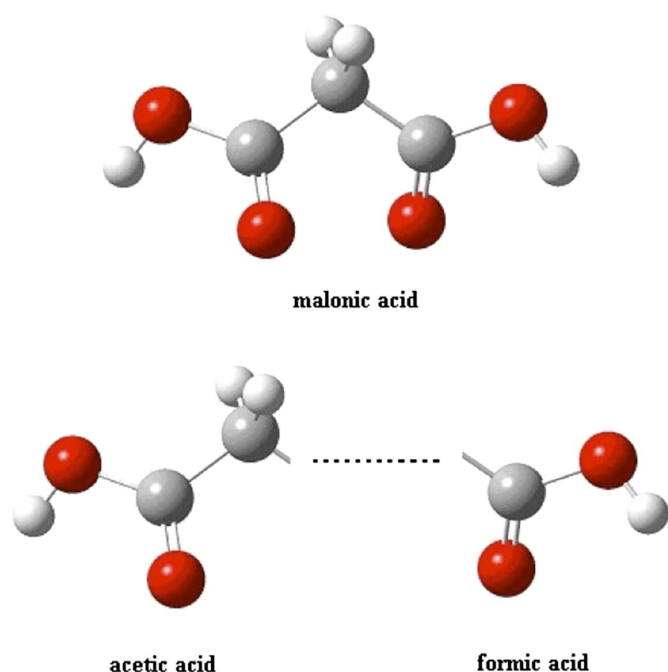


Fig. 1. Ball and stick model of malonic acid. Grey spheres are carbon atoms, red spheres are oxygen atoms and white spheres are hydrogen atoms. Also shown is malonic acid split into two other molecules, acetic acid and formic acid (with the dangling bond on each representing the necessary proton). (For interpretation of the references to colour in this figure legend, the reader is referred to the web version of this article.)

integrity of these bonds could lead to a loss of the charge transfer route from the dye into the TiO_2 . It has been shown by O'Shea et al. [18] that the ligand used in the N3 dye, bi-isonicotinic acid, is damaged under synchrotron radiation resulting in the bi-isonicotinic acid molecules splitting into two isonicotinic acid molecules. Similar results were found for glycine adsorbed on the rutile TiO_2 (110) surface [5,19]. These observations may raise questions about the design of new high flux beamlines on 3rd generation synchrotron sources for the study of these molecules and measures that may be required to reduce these problems.

This paper presents photoemission spectra and NEXAFS spectra to investigate the adsorption of malonic acid on the rutile TiO_2 (110) surface. The molecular adsorption is studied using NEXAFS and photoelectron spectroscopy in order to determine the bonding geometry and mode of bonding. In addition, a comparison of the stability of the adsorbed malonic acid is made by carrying out photoelectron spectroscopy measurements on a bending magnet beamline and comparing these to work carried out on an insertion device beamline.

2. Experimental

The experiments were carried out on beamline D1011 ($40 \text{ eV} \leq h\nu \leq 1500 \text{ eV}$) at MAX-lab, Sweden, and beamline MPW6.1 ($30 \text{ eV} \leq h\nu \leq 350 \text{ eV}$) at SRS Daresbury Laboratory, UK. Beamline D1011 [20] is a bending magnet beamline with a photon flux of 10^{10} – $10^{11} \text{ photons s}^{-1}$ and beamline MPW6.1 was a wiggler insertion device beamline [21] with a photon flux of 10^{12} – $10^{13} \text{ photons s}^{-1}$ over the photon energy range used in these measurements. The endstation of beamline D1011 is equipped with a Scienta SES200 hemispherical analyser with an angular acceptance angle of $\pm 6^\circ$.

The rutile TiO_2 (110) crystal (Pi-kem Ltd.) was cut and epi-polished on one side to within 0.2° of the (110) plane. The crystal was prepared by repeated cycles of 1 keV Ar^+ ion etching and annealing to 750°C in vacuum until XPS spectra showed no contamination and a sharp (1×1) LEED pattern was obtained [22]. Malonic acid powder ($>99\%$, Fluka) was degassed in an evaporating arm for 1 h by heating to

$\sim 100^\circ \text{C}$. Malonic acid decomposes at 135°C so care was taken not to heat the acid to temperatures higher than this. To dose the TiO_2 with malonic acid the temperature of the tantalum envelope containing the powder was reduced to 80 – 95°C , whilst the TiO_2 crystal was held at room temperature (*ca.* 23°C). For the measurements carried out on MPW6.1 of the SRS the rutile TiO_2 (110) surface was subjected to multiple exposures (ranging from 1 to 15 min, equivalent to *ca.* 0.6 – 100 L) of malonic acid but no evidence of multilayer formation was observed. In the measurements performed on beamline D1011 at MAX-Lab, the rutile TiO_2 (110) crystal was exposed to malonic acid for approximately 15 min (equivalent to *ca.* 100 L).

Photoemission and NEXAFS data were recorded from the rutile TiO_2 (110) surface before and after evaporation of malonic acid. Photoemission spectra were recorded at normal emission, with the incident beam at 40° to the surface normal. Clean and dosed spectra were aligned on the binding energy scale using Fermi edges recorded from the tantalum sample clips. Binding energies are quoted to $\pm 0.1 \text{ eV}$. Peak fitting of the photoelectron spectroscopy data was performed using CasaXPS software. A Shirley background was subtracted from the photoemission data. Voigt curves (70% Gaussian: 30% Lorentzian) were used to fit the core level photoemission spectra. Photoemission spectra are normalised to the incident photon flux unless stated otherwise.

3. Results

3.1. Characterisation of the adsorption mode of malonic acid on rutile TiO_2 (110)

We begin by discussing the spectra recorded on the bending-magnet beamline D1011 at MAX-lab. Fig. 2 shows the O 1s spectra for clean rutile TiO_2 (110) and for malonic-acid-dosed rutile TiO_2 (110) recorded at a photon energy of 700 eV . The O 1s spectrum recorded from the clean surface is fitted with a single peak at 530.4 eV . This is attributed to the oxygen atoms in the TiO_2 crystal [23]. Following adsorption of malonic acid on TiO_2 , the O 1s spectrum can be fitted with three peaks at binding energies as shown in Table 1. The first peak is assigned to the oxygen atoms in the TiO_2 surface [23] and is at a similar binding energy to the corresponding peak in the clean spectrum. The second peak at 532.0 eV is assigned to carboxyl oxygen atoms in the molecule [24]. There are four oxygen atoms in each malonic acid molecule, which are not equivalent (two are carbonyl and two are hydroxyl oxygen species). If the molecule adsorbs on the surface in a twice-bidentate bridging structure (bonding through all 4 oxygen atoms following deprotonation of both acid groups) to form malonate shown in Fig. 2b, then all of the oxygen atoms will be in the same chemical environment, resulting in one peak in the spectrum [25]. The O 1s spectrum recorded upon adsorption of the malonic acid strongly suggests that the molecule is indeed doubly deprotonated and adsorbs in a twice-bidentate geometry following deprotonation of the acid groups, as shown schematically in Fig. 2c. The third, rather weak peak, at a binding energy of 533.9 eV may arise from a small number of intact carboxyl group OH species, for example if some fraction of the molecules are adsorbed in a monodentate geometry [26] (Fig. 2d) and therefore adsorbed only through a single carboxylate group (Fig. 2e). It is also possible that this peak arises from a small number of molecules not bonded to the surface, for example forming the beginnings of a second layer of malonic acid. Table 1 shows the binding energies, percentage of total O 1s signal and summarises the assignment of peaks fitted to the O 1s spectra for clean rutile TiO_2 (110) and for malonic-acid-dosed rutile TiO_2 (110). What is clear from these data is that the majority of the malonic acid is adsorbed in a doubly bidentate mode following deprotonation of the carboxyl groups.

Fig. 3 shows the Ti 2p spectra recorded at a photon energy of 1000 eV for clean rutile TiO_2 (110) and following adsorption of malonic acid normalised to the intensity of the Ti $2p_{3/2}$ peak. Table 2 summarises the binding energies, percentage of total Ti 2p signal and origins of the peaks [27,28] fitted to the Ti 2p spectra for clean rutile TiO_2 (110) and

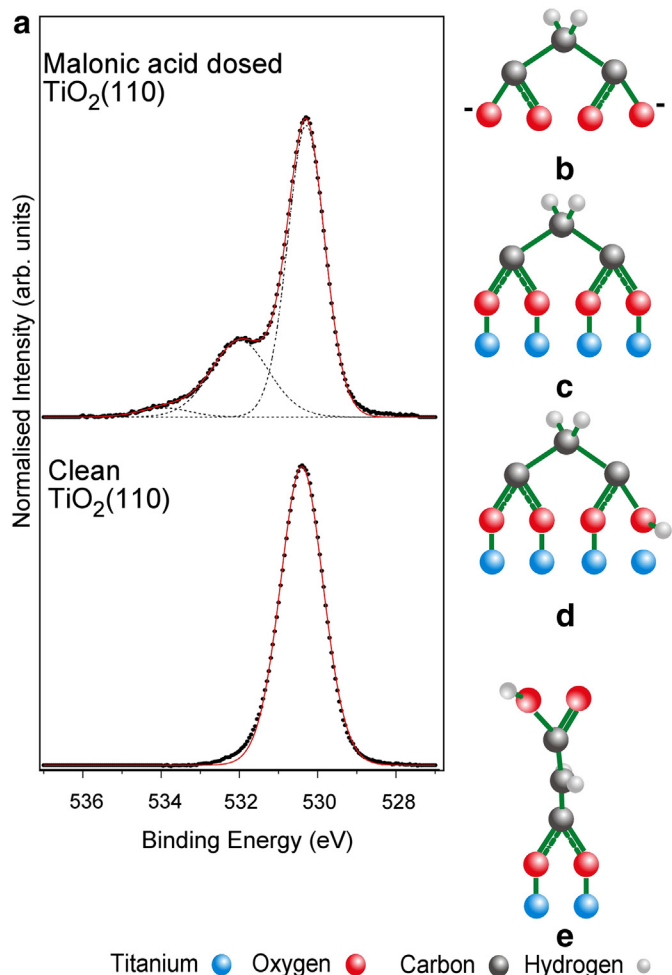


Fig. 2. a) O 1s spectra for clean rutile TiO₂ (110) and malonic-acid-dosed rutile TiO₂ (110) recorded at a photon energy of 700 eV. The black dots are the experimental data, the red line is the total fit to the data and the dashed lines are the components fitted to the data. b) Schematic of doubly deprotonated malonate ion. c) Doubly-bidentate bridging adsorption mode of malonate. d) Singly-bidentate/monodentate bridging adsorption mode of malonate. e) Singly bidentate adsorption mode of malonic acid. (For interpretation of the references to colour in this figure legend, the reader is referred to the web version of this article.)

for malonic-acid-dosed rutile TiO₂ (110). The presence of the Ti³⁺ derived peak is widely attributed to O-bridging oxygen vacancies on the surface [29]. The data show that there is no shift in the binding energy of the Ti 2p_{3/2} peak suggesting that there is no malonic-acid-induced band-bending following adsorption in contrast to the adsorption of similar molecules such as dopamine [30] and catechol [31] on anatase and rutile TiO₂ surfaces. In addition, Table 2 shows that there is very little change in the intensity of the Ti³⁺ derived peaks indicating that adsorption of the molecule does not lead to ‘healing’ of the O-bridging vacancies.

Table 1
Binding energies, percentage of total O 1s signal (in brackets) and origin of peaks fitted to the O 1s spectra of clean rutile TiO₂ (110) and malonic-acid-dosed rutile TiO₂ (110).

Binding energy (eV)		
Clean rutile	Malonic-acid-dosed rutile	Origin of peak
530.4 (100%)	530.3 (69.0 ± 0.7%)	Oxygen atoms in TiO ₂ surface [23]
	532.0 (28.1 ± 1.5%)	Carboxyl oxygen atoms [24]
	533.9 (2.9 ± 2.1%)	Molecule hydroxyl groups [43]

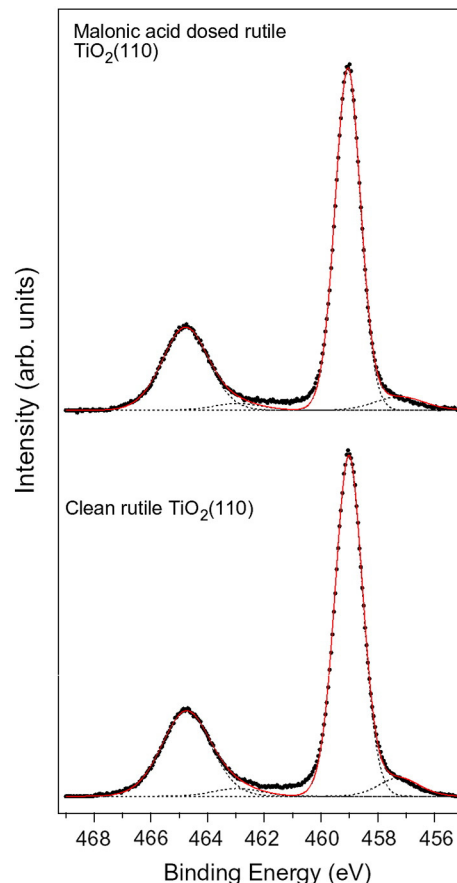


Fig. 3. Ti 2p spectra of clean rutile TiO₂ (110) and malonic-acid-dosed rutile TiO₂ (110) recorded at a photon energy of 700 eV. The black dots are the experimental data, the red line is the total fit to the data and the dashed lines are the components fitted to the data. (For interpretation of the references to colour in this figure legend, the reader is referred to the web version of this article.)

Table 2 also gives the intensities of the Ti 2p_{3/2} peak before and after dosing with malonic acid. A rough approximation of the surface coverage can be obtained from these values using the equation,

$$I_d = I_c(1 - \phi_A + \phi_A \exp(-d/\lambda \cos \theta)) \quad [28], \quad (1)$$

where, I_d is the intensity of the Ti 2p_{3/2} peak of the dosed surface and I_c for the clean surface, ϕ_A is the surface coverage, d is the ‘diameter’ of the molecule, λ is the inelastic mean free path (IMFP) and θ is the angle of the incident X-ray beam relative to the surface normal (40°). Using the measured change in the intensity of the Ti 2p_{3/2} peak (I_d/I_c) of 0.63, the IMFP of TiO₂ of 1.7 nm [32] and taking an approximate ‘diameter’ of the malonic acid molecule to be 10 Å, we obtain a coverage of 0.26. This would suggest that there is roughly one molecule for every four five-fold coordinated Ti atoms (Ti_{5c}) at the surface. This supports the doubly-bidentate adsorption geometry inferred by the O 1s spectrum following adsorption of malonate.

Fig. 4 shows the C 1s spectrum for malonic-acid-dosed rutile TiO₂ (110) recorded at a photon energy of 350 eV on the bending magnet beamline D1011. This was recorded following dosing with 100 L malonic acid. The spectrum can be fitted with two peaks at binding energies of 285.9 eV (42.0 ± 1.0%) and 289.5 eV (58.0 ± 0.8%). The two fitted peaks are assigned to CH₂ and COO[−] carbon atoms respectively [24,28]. The full width half maxima of the peaks in this spectrum are 1.95 eV (CH₂) and 1.8 eV (COO[−]) in reasonable agreement with adsorption of acetate on the rutile TiO₂ (011) surface [28]. The Voigt peaks fitted to the C 1s spectrum have a ratio of 1:1.4 (±0.1), which is not what would be expected from malonate (1:2). The reason for the

Table 2Binding energies, percentage of total Ti 2p signal (in brackets) and origin of peaks fitted to the Ti 2p spectra of clean rutile TiO₂ (110) and malonic-acid-dosed rutile TiO₂ (110).

Binding energy (eV)		
Clean rutile	Malonic acid adsorbed on rutile	Origin of peak
457.3 (5.1 ± 3.4%)	457.2 (4.9 ± 3.5%)	Ti ³⁺ : 2p _{3/2} component [27]
459.0 (63.9 ± 1.4%) intensity (arb. units) = 18,574	459.1 (64.4 ± 1.6%) Intensity (arb. units) = 11,702	Ti ⁴⁺ : 2p _{3/2} component [28]
463.0 (2.6 ± 2.1%)	462.9 (2.5 ± 2.2%)	Ti ³⁺ : 2p _{1/2} component [27]
464.8 (28.4 ± 2.6%)	464.8 (28.2 ± 3.1%)	Ti ⁴⁺ : 2p _{1/2} component [28]

deviation from the expected stoichiometric ratio of the two C derived peaks for malonate is not clear. It may be due to photoelectron effects, since the carboxylate carbon is closer to the surface than the central alkyl carbon then the photoemitted electron wave is more likely to be diffracted due to backscattering from the underlying surface [33]. Previous work on using this analyser in a normal emission geometry has also shown deviations from stoichiometry for the atoms closest to the surface [34]. However in the absence angle-resolved or energy-resolved photoelectron diffraction measurements this is not certain for the current case. A comparison of a “survey” C 1s spectrum (recorded with a step size of 0.5 eV) and the spectrum shown in Fig. 4, which was recorded 30 min after the wide scan shows no significant change in the intensity or width of the two peaks (see Supplementary information Fig. S1). This suggests that the molecule is stable under synchrotron radiation on beamline D1011 for the duration of the measurements made on D1011 at MAXlab. The deviation from stoichiometry for the C 1s however does not rule out the possibility that some dissociation or reaction has occurred at the surface prior to exposure to the beam. The most obvious decomposition reaction for this molecule would be the formation of acetate and formate by scission at the CH₂ group as shown in Fig. 1. However this would not change the overall COO:CH₂

ratio. Loss of the CH₂ group would of course lead to an increase in the relative amount of COO, which is not consistent with the C 1s spectrum. Another possibility, which would be consistent with the data, would be adsorption through only one carboxylate and subsequent loss of the second carboxylate group as CO₂. The latter is a slow reaction at 90 °C in aqueous solution at low pH, and becomes even slower at pH > 4 [35] thus we expect it to be unlikely in vacuum. During deposition, great care was taken to keep the temperature low, and, in the absence of water, so we expect little decomposition to have occurred although of course this can never be completely ruled out.

Fig. 5a shows carbon K-edge NEXAFS spectra from a malonic acid-dosed rutile TiO₂ (110) surface, recorded with the electric vector of the incident synchrotron radiation (SR) beam along the [001] azimuth. The incident angle of the SR beam was varied from 20° to 90° relative to the sample surface. The spectrum with the SR beam at 90° to the surface (normal incidence) was recorded immediately following exposure of the surface to around 100 L of malonic acid. In all of the spectra, a sharp peak is observed at a photon energy of 288.8 ± 0.2 eV and a broad resonance centred around 301 eV is also clearly visible. The energies and line shapes of these features are all in good agreement with those recorded for NEXAFS spectra of formate, acetate and propionate adsorbed on rutile TiO₂ (110) recorded by Gutiérrez-Sosa et al. [17]. The sharp peak at 288.8 ± 0.2 eV is assigned to C 1s → π* excitations in the carboxylate groups. If both carboxylate groups bond to surface titanium atoms in a bidentate structure, as suggested by the O 1s photoelectron spectrum, the carboxyl carbon atoms should produce one main π* resonance as we observe here. The broad resonance at around 301 eV is attributed to C 1s → σ* transitions.

Malonate would be expected to give rise to a similar shaped spectrum to acetate but the intensity of the π* resonance relative to the σ* resonances (broad higher energy features) should be twice as large given the same angle of incident light on the sample. This is because according to the building block principle, the NEXAFS spectrum of a molecule should be a linear combination of the individual spectra of its functional groups or bonds [36]. Although it seems that the relative intensity of the π*-derived peak to the σ* derived peak is larger in this work compared to the corresponding spectrum for acetate from ref. 15, a definitive comparison is not possible due to the variation in the intensity of the peaks with the incident photon angle. The angle-resolved NEXAFS data recorded with the electric vector of the incident X-ray beam along the [001] azimuth seem to show some angular dependence, as shown in Fig. 5b. Fitting of the Stohr equations [37] gives a tilt angle of the C=O groups of 56° ± 10°. However, the angle derived for the molecular tilt (i.e. the tilt of the carboxylate groups relative to the surface normal) of 56° is close to the ‘magic angle’ of 54.7° [37]. This means that we are unable to unambiguously determine whether the molecules are ordered on the surface. A lack of ordering may be due to decomposition of the molecule under the synchrotron radiation beam, although on the bending-magnet beamline we did not observe any changes to suggest decomposition of the molecule. The O 1s spectra suggest that a small number of the molecules may in fact be adsorbed in a singly bidentate geometry, which would leave the other carboxyl group free to rotate around the central C atom; sterically, and electrostatically one would perhaps expect the two carboxyl groups to be orthogonal to one another. The presence of some singly bidentate adsorbed species would give rise to a minority species with the π* vector at some other

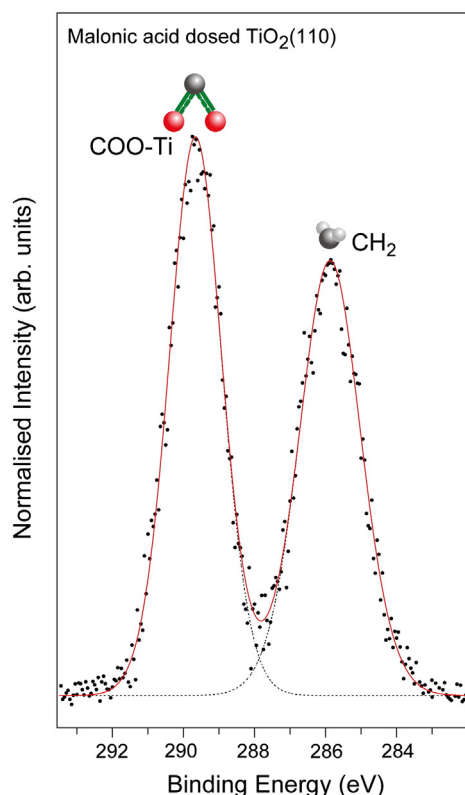


Fig. 4. C 1s spectra of clean rutile TiO₂ (110) and malonic-acid-dosed rutile TiO₂ (110) recorded at a photon energy of 1000 eV. The black dots are the experimental data, the red line is the total fit to the data and the dashed lines are the components fitted to the data. (For interpretation of the references to colour in this figure legend, the reader is referred to the web version of this article.)

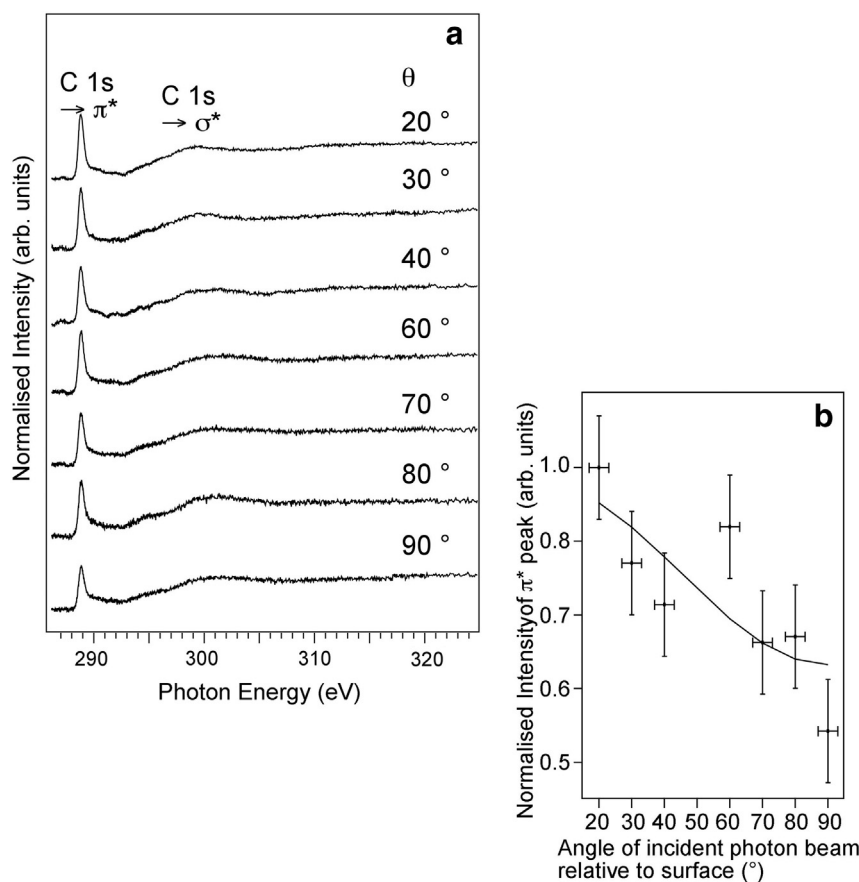


Fig. 5. a) Angle-resolved carbon K-edge NEXAFS spectra of malonic-acid-dosed rutile TiO_2 (110). θ is the angle of the incident radiation relative to the surface. b) Intensity of the π^* peak as a function of incident angle relative to the surface. The markers are the experimental data and the line a fit using the Stöhr equations [37].

angle relative to the bonded carboxylate groups. A third possibility for the apparent lack of order is the bonding geometry of the carboxylate groups with respect to the azimuthal geometry of the crystal. This latter would occur if the molecules are oriented with the π^* vector of the bonded carboxylate groups along the $[1\bar{1}0]$ azimuth. In this situation no angular variation would be observed in the NEXAFS spectra [37] obtained by rotating the polar angle. Unfortunately, angle-resolved NEXAFS spectra could not be recorded along the $[1\bar{1}0]$ azimuth due to limitations of the sample manipulator.

The O 1s photoemission data suggest that the majority of the molecules are adsorbed in a doubly bidentate mode following loss of the proton from both carboxylic acid groups. Fig. 6 shows a schematic of two possible adsorption geometries, which are consistent with the data. The molecule–surface ($\text{Ti}_{\text{surface}} - \text{O}_{\text{molecule}}$) bond lengths used for the bridging geometry shown in Fig. 6b is 2 Å. This is consistent with bond length deduced from photoelectron diffraction measurements for formate adsorption in a bidentate bridging mode on this surface [38]. As discussed above it was not possible to obtain the azimuthal angle from the NEXAFS data, thus it is not possible to determine which of these structures is most likely from our data. However, most studies of carboxylic acid adsorption on rutile TiO_2 (110) surfaces in ultra-high vacuum suggest a bridging bidentate geometry to be favoured [16] as shown in Fig. 6b. The figure suggests that the molecule would in theory be able to bond across the bridging oxygen rows since the central carbon atom is likely to coincide with the valley between two neighbouring bridging oxygen atoms (O_{br}).

It is well known that O-vacancies can easily be produced at the rutile TiO_2 (110) surface by electron or ion bombardment. As mentioned above on the rutile TiO_2 (110) surface oxygen is thought to be lost from the bridging oxygen rows. The intensity of the Ti 2p component associated with Ti^{3+} allows us to estimate that the concentration of

oxygen vacancies at the TiO_2 (110) surface is rather low, *ca.* $4 \pm 3\%$ [39,40]. It is clear that our measurement characterises the adsorption of malonic acid at a largely undefected surface. The Ti 2p spectra discussed above do not show any change in the intensity of the Ti^{3+} derived peak upon adsorption of the malonic acid. It is possible that the presence of O-vacancies in a more highly defected surface may lead to a change in the adsorption mechanism at the vacancy sites. Indeed DFT calculations for dopamine adsorbed on anatase surfaces suggested the molecule adsorbed preferentially in a chelating mode (i.e. both O atoms bonded to a single surface Ti) at O-vacancy sites [41]. The absence of a change in the intensity of the Ti^{3+} derived peak in the Ti 2p spectra does not rule this possibility out for the current study since it is well known from water adsorption studies that although water adsorbs at O-vacancies, Ti^{3+} is not removed from the surface [29]. With regard to the effect of O-vacancy concentration on molecular adsorption at the rutile TiO_2 (110) surface generally, there is still some debate. It would therefore be interesting to probe the effect of the surface O-vacancy concentration of TiO_2 on the adsorption of malonic acid.

3.2. Synchrotron radiation induced beam damage of malonic acid on rutile TiO_2 (110)

Fig. 7 shows the C 1s photoelectron spectra following a 15 minute dose of malonic acid at 90 °C (*can* 100 L), recorded at a photon energy of 350 eV on the insertion device beamline, MPW6, at the Daresbury SRS. The spectra can be fitted with two peaks at binding energies of 285.9 eV and 289.7 eV, which again are assigned to CH_2 and COO^- carbon atoms in the molecule [28]. A number of core level and valence band spectra were recorded over a period of a few hours before the beam was shut off for 12 h and the spectrum was recorded again, as

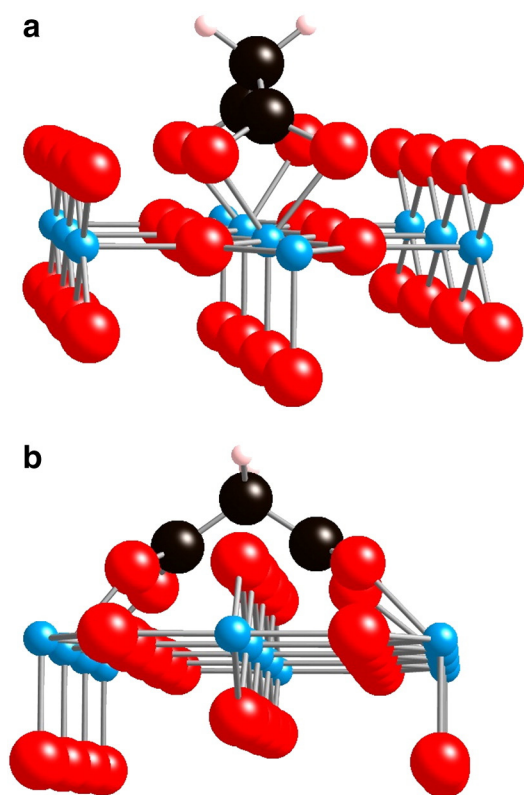


Fig. 6. Schematic ball and stick diagrams of two possible bonding modes of malonate on rutile TiO_2 (110) which involves dissociation of both carboxylate groups upon adsorption. (a) doubly bidentate chelating mode along the [001] 5-fold co-ordinated Ti atoms and (b) Doubly bidentate bridging adsorption along the [110] direction crossing the bridging oxygen rows. Red 'spheres' represent oxygen atoms, blue is titanium, white is hydrogen and black is carbon. The $\text{Ti}_{\text{surface}} - \text{O}_{\text{molecule}}$ bond lengths are set to 2 Å in both cases.

shown in Fig. 7 (curve b). This spectrum was recorded from a slightly different location on the crystal. The C 1s spectrum was then recorded again (c) 7 min and (d) 12 min after spectrum (b). The position of the beam on the crystal was then moved again and the C 1s spectrum recorded is shown in Fig. 7 (curve e). C 1s spectra were then recorded (f) 3 min, (g) 15 min, (h) 34 min and (i) 53 min after spectrum (e) with the sample constantly exposed to the soft X-ray beam. On the new location on the crystal, the peak at 289.7 eV is a similar height to the lower binding energy peak but slowly reduces in intensity with time spent under the X-ray beam. The change in the peak areas of the C 1s components is also shown in Fig. 7. It can be seen clearly that the higher binding energy peak area decreases, accompanied by an increase in the area of the lower energy peak, which might indicate the conversion of COO to CH_2/CH_3 groups at the surface. Over a period of 12 min ((c) and (d) in Fig. 7), following spectrum (b) there is very little change in the peak area of the CH-derived peak. The COO derived peak undergoes a further loss of intensity after 7 min but does not change between 7 and 12 min. When the beam position is moved on the sample surface, there is an increase in both peak areas (point (e)). However, Table 3 shows that moving to a new position on the crystal does not result in a return to the original 1:1.4 ratio of the alkyl:carboxyl peak intensity. Continued exposure of the surface (points (f)–(i)) to the high flux beam leads to a decrease in the areas of both peaks suggesting that the molecules are being desorbed from the surface. The ratio of the areas of the peaks at 289.5 eV and 289.7 eV binding energy remains roughly constant over this range, suggesting that both species are lost together. In addition to the change in intensity of the two peaks, we note that both peaks become broadened relative to the spectrum recorded in Fig. 7. This may be due to the formation of a mixture of molecules at the surface caused by decomposition of the malonate species. One may expect that there would be a slight downward shift in the binding energy of the alkyl carbon in acetate or formate relative to malonate, due to the extra carboxyl group in malonate. The decomposition of malonic acid seems to have occurred much more rapidly in

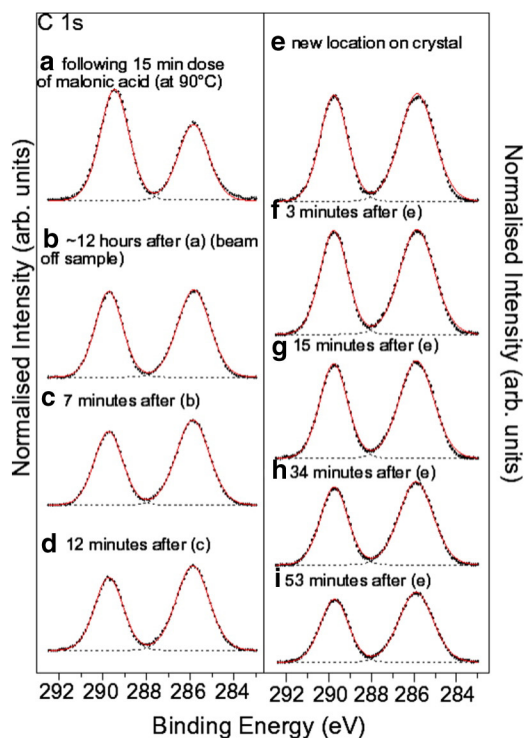


Fig. 7. Left panels: (a)–(i) C 1s spectra of malonic-acid-dosed rutile TiO_2 (110) recorded at a photon energy of 350 eV. The black dots are the experimental data, the red line is the total fit to the data and the dashed lines are the components fitted to the data. Right panel: Integrated peak areas of the C 1s peaks at 289.5 eV (red open circles) and 285.9 eV (blue filled squares). (For interpretation of the references to colour in this figure legend, the reader is referred to the web version of this article.)

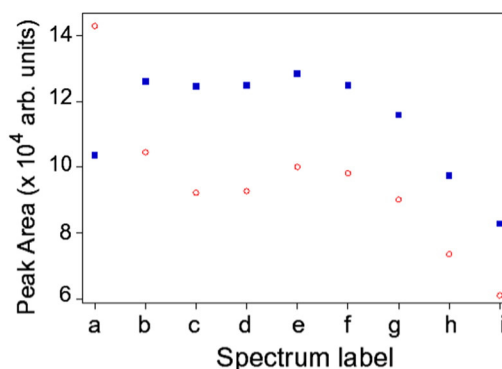


Table 3

The ratio of areas of the fitted peaks at 285.9 eV and 289.7 eV binding energy in Fig. 6(a)–(i).

Fig. 7	(a)	(b)	(c)	(d)	(e)	(f)	(g)	(h)	(i)
Ratio of peak areas at 285.9:289.7 eV binding energy	1:1.4	1:0.8	1:0.7	1:0.7	1:0.8	1:0.8	1:0.8	1:0.8	1:0.7

the work carried out on MPW6.1 of the SRS than on D1011 at MAX-lab. If one considers the power falling on the samples based on the flux and the fact the D1011 beam spot size is roughly $3 \text{ mm} \times 1 \text{ mm}$ and that on MPW6.1 was roughly $0.6 \text{ mm} \times 0.3 \text{ mm}$ then one has roughly between 20 and 2000 times the power incident on the sample on the MPW6.1 beamline.

The data above seem to suggest the decomposition of the malonic acid under the high flux MPW6.1 beamline, most probably to form acetate on the surface by spitting of the malonate as shown in Fig. 1. The relative intensity of the COO^- to CH_3 peaks of around 0.8 is similar to that obtained by Quah et al. for acetic acid adsorption on this surface [28]. The formation of acetate from malonic acid is at odds with the ATR-IR study mentioned above, which suggests that the majority species adsorbed at the surface, formed by decomposition of malonic acid, is oxalate [42]. The difference here probably lies in the fact that the current study is carried out in ultra-high vacuum. The reaction scheme to form oxalate suggested in Ref. [42] involves both CO_2 and O_2 species. In vacuum we suspect that although CO_2 may be generated by the beam-induced decomposition of malonic acid, it would be lost from the surface. In addition, the background oxygen level in UHV is simply not sufficient to drive substantial formation of oxalate. The results do, however, seem to support the photo-induced formation of an intermediate acetate moiety in the decomposition process as suggested in Ref. [42].

4. Conclusions

Photoelectron and NEXAFS spectroscopies have been used to study the interaction of malonic acid with a relatively defect-free rutile TiO_2 (110) surface. O 1s core-level photoelectron spectra recorded from a freshly deposited monolayer of malonic acid suggest that the majority of the molecules adsorb in a doubly-bidentate geometry to four Ti_{5c} atoms, i.e. both carboxyl groups appear to bond via deprotonation. Angle-resolved NEXAFS spectra suggest the $\text{C}=\text{O}$ groups are tilted $56^\circ \pm 10^\circ$ from the surface normal and that the molecule remains intact upon adsorption. Unfortunately the azimuthal orientation of the molecule could not be determined from the NEXAFS data. It is also found that the adsorbed molecule is unstable under soft X-ray radiation on an insertion device beamline. The XPS spectra recorded over several hours suggest decomposition to form acetate, although there may also be other species such as formate and intact malonic acid on the surface.

Supplementary data to this article can be found online at <http://dx.doi.org/10.1016/j.susc.2014.03.015>.

Acknowledgements

The authors are grateful to the support from the I3 IA-SFS programme, funded by EU FP6, to carry out the experimental work at MAX-lab, the Swedish Research Council, and STFC to fund experimental work at the SRS. KLS and BFS acknowledge the support from EPSRC and STFC for studentships. MJJ is funded through the NowNano Doctoral Training Centre (EPSRC(UK) grant EP/G03737X/1).

The authors would like to dedicate this paper to Paul Wincott, who sadly passed away in August 2013. Paul was a mentor to AGT during his PhD studies and a collaborator with AGT, WRF and VRD.

References

- [1] G.J. Fleming, K. Adib, J.A. Rodriguez, M.A. Barteau, J.M. White, H. Idriss, *Surf. Sci.* 602 (2008) 2029.
- [2] S. Köppen, O. Bronkalla, W. Langel, *J. Phys. Chem. C* 112 (2008) 13600.
- [3] A.G. Thomas, W.R. Flavell, C.P. Chatwin, A.R. Kumarasinghe, S.M. Rayner, P.F. Kirkham, D. Tsoutsou, T.K. Johal, S. Patel, *Surf. Sci.* 601 (2007) 3828.
- [4] R. Tonner, *ChemPhysChem* 11 (2010) 1053.
- [5] E. Soria, I. Colera, E. Roman, E.M. Williams, J.L. de Segovia, *Surf. Sci.* 451 (2000) 188.
- [6] B. O'Regan, M. Grätzel, *Nature* 353 (1991) 737.
- [7] H. Rensmo, K. Westermark, S. Sodergren, O. Kohle, P. Persson, S. Lunell, H. Siegbahn, *J. Chem. Phys.* 111 (1999) 2744.
- [8] M.K. Nazeeruddin, A. Kay, I. Rodicio, R. Humphrybaker, E. Muller, P. Liska, N. Vlachopoulos, M. Grätzel, *J. Am. Chem. Soc.* 115 (1993) 6382.
- [9] G. Boschloo, J. Lindstrom, E. Magnusson, A. Holmberg, A. Hagfeldt, *J. Photochem. Photobiol. A Chem* 148 (2002) 11.
- [10] M.K. Nazeeruddin, P. Pechy, T. Renouard, S.M. Zakeeruddin, R. Humphry-Baker, P. Comte, P. Liska, L. Cevey, E. Costa, V. Shklover, et al., *J. Am. Chem. Soc.* 123 (2001) 1613.
- [11] V. Aranyos, H. Grennberg, S. Tingry, S.E. Lindquist, A. Hagfeldt, *Sol. Energy Mater. Sol. Cells* 64 (2000) 97.
- [12] A. Fujishima, K. Honda, *Nature* 238 (1972) (37–+).
- [13] K. Kalyanasundaram, M. Grätzel, *Curr. Opin. Biotechnol.* 21 (2010) 298.
- [14] D.S. Bhatkhande, V.G. Pangarkar, A. Beenackers, *J. Chem. Technol. Biotechnol.* 77 (2002) 102.
- [15] C.L. Pang, R. Lindsay, G. Thornton, *Chem. Soc. Rev.* 37 (2008) 2328.
- [16] A. Thomas, K. Syres, *Chem. Soc. Rev.* 41 (2012) 4207.
- [17] A. Gutierrez-Sosa, P. Martinez-Escobedo, H. Raza, R. Lindsay, P.L. Wincott, G. Thornton, *Surf. Sci.* 471 (2001) 163.
- [18] J.N. O'Shea, J. Ben Taylor, L.C. Mayor, J.C. Swarbrick, J. Schnadt, *Surf. Sci.* 602 (2008) 1693.
- [19] E. Soria, E. Roman, E.M. Williams, J.L. de Segovia, *Surf. Sci.* 433 (1999) 543.
- [20] R. Nyholm, S. Svensson, J. Nordgren, A. Flodstrom, *Nucl. Instrum. Methods Phys. Res. Sect. A-Accel. Spectrom. Dect. Assoc. Equip.* 246 (1986) 267.
- [21] M. Bowler, J.B. West, F.M. Quinn, D.M.P. Holland, B. Fell, P.A. Hatherly, I. Humphrey, W.R. Flavell, B. Hamilton, *Surf. Rev. Lett.* 9 (2002) 577.
- [22] A.G. Thomas, W.R. Flavell, A.R. Kumarasinghe, A.K. Mallick, D. Tsoutsou, G.C. Smith, R. Stockbauer, S. Patel, M. Grätzel, R. Hengerer, *Phys. Rev. B* (2003) 67.
- [23] N.P. Huang, R. Michel, J. Voros, M. Textor, R. Hofer, A. Rossi, D.L. Elbert, J.A. Hubbell, N.D. Spencer, *Langmuir* 17 (2001) 489.
- [24] H.K. Lee, K.J. Kim, J.H. Han, T.H. Kang, J.W. Chung, B. Kim, *Phys. Rev. B* 77 (2008) (115324–115321–115324–115324).
- [25] J. Schnadt, J.N. O'Shea, L. Patthey, J. Schiessling, J. Krempasky, M. Shi, N. Mårtensson, P.A. Bruhwiler, *Surf. Sci.* 544 (2003) 74.
- [26] I. Dolamic, T. Burgi, *J. Phys. Chem. B* 110 (2006) 14898.
- [27] G.J. Fleming, K. Adib, J.A. Rodriguez, M.A. Barteau, H. Idriss, *Surf. Sci.* 601 (2007) 5726.
- [28] E.L. Quah, J.N. Wilson, H. Idriss, *Langmuir* 26 (2010) 6411.
- [29] C.M. Yim, C.L. Pang, G. Thornton, *Phys. Rev. Lett.* 104 (2010) 259704.
- [30] K. Syres, A. Thomas, F. Bondino, M. Malvestuto, M. Grätzel, *Langmuir* 26 (2010) 14548.
- [31] K.L. Syres, A.G. Thomas, W.R. Flavell, B.F. Spencer, F. Bondino, M. Malvestuto, A. Preobrajenski, M. Grätzel, *J. Phys. Chem. C* 116 (2012) 23515.
- [32] G.G. Fuentes, E. Elizalde, F. Yubero, J.M. Sanz, *Surf. Interface Anal.* 33 (2002) 230.
- [33] D.P. Woodruff, *J. Electron Spectrosc. Relat. Phenom.* 100 (1999) 259.
- [34] A.B. Preobrajenski, A.S. Vinogradov, M.L. Ng, E. Čavar, R. Westerström, A. Mikkelsen, E. Lundgren, N. Mårtensson, *Phys. Rev. B* 75 (2007) 245412.
- [35] G.A. Hall, *J. Am. Chem. Soc.* 71 (1949) 2691.
- [36] K. Kaznacheyev, A. Osanna, C. Jacobsen, O. Plashkevych, O. Vahtras, H. Agren, *J. Phys. Chem. A* 106 (2002) 3153.
- [37] J. Stöhr, *NEXAFS Spectroscopy*, Springer-Verlag, Berlin, 2003.
- [38] D.I. Sayago, M. Polcik, R. Lindsay, R.L. Toomes, J.T. Hoelt, M. Kittel, D.P. Woodruff, *J. Phys. Chem. B* 108 (2004) 14316.
- [39] A.G. Thomas, W.R. Flavell, A.K. Mallick, A.R. Kumarasinghe, D. Tsoutsou, N. Khan, C. Chatwin, S. Rayner, G.C. Smith, R.L. Stockbauer, et al., *Phys. Rev. B* 75 (2007) 035105.
- [40] S. Wendt, J. Matthiesen, R. Schaub, E.K. Vestergaard, E. Laegsgaard, F. Besenbacher, B. Hammer, *Phys. Rev. Lett.* 96 (2006).
- [41] M. Vega-Arroyo, P.R. LeBreton, T. Rajh, P. Zapol, L.A. Curtiss, *Chem. Phys. Lett.* 406 (2005) 306.
- [42] I. Dolamic, T. Burgi, *Catal.* 248 (2007) 268.
- [43] J. Ben Taylor, L.C. Mayor, J.C. Swarbrick, J.N. O'Shea, J. Schnadt, *J. Phys. Chem. C* 111 (2007) 16646.